Available online at www.sciencedirect.com
ScienceDirect
Trans. Nonferrous Met. Soc. China 30(2020) 823−834
Transactions of Nonferrous Metals Society of China
www.tnmsc.cn

Aluminium electrodeposition under novel conditions from $AlCl_3$−urea deep eutectic solvent at room temperature

Vesna S. CVETKOVIĆ[1], Nataša M. VUKIĆEVIĆ[1], Niko JOVIĆEVIĆ[2],
Jasmina S. STEVANOVIĆ[1], Jovan N. JOVIĆEVIĆ[1]

1. Institute of Chemistry, Technology and Metallurgy, National Institute,
Department of Electrochemistry, University of Belgrade, Belgrade, Serbia;
2. Nissan Technical Center North America, Inc., 39001 Sunrise Drive, Farmington Hills, MI 48331-3487, USA

Received 23 May 2019; accepted 10 November 2019

Abstract: The electrodeposition of aluminium on glassy carbon and aluminium substrates from $AlCl_3$−urea deep eutectic solvent (DES) system at near room temperatures was investigated, without additional purification of the chemicals used to prepare the electrolyte and without rigorous control of moisture and oxygen present in the working space. The effects of changing temperature, working potential, controlled deposition current density and deposition time on the morphology of deposited aluminium without stirring of the electrolyte were recorded. Using potentiostatic and galvanostatic techniques, aluminium was electrodeposited from the deep eutectic solvent ($n(AlCl_3):n(\text{urea})=1.6:1$) onto glassy carbon and aluminium substrates at temperatures ranging from 25 to 50 °C. Using SEM, EDS and XRD techniques, substrates were studied and confirmed the presence of aluminium deposits following both potentiostatic and galvanostatic regimes. The shape and size of Al grains deposited depended on the time of deposition and varied in size from nanometers to micrometers and in shape from regular crystal forms to needle-like and flake-like structures.

Key words: aluminium; electrodeposition; deep eutectic solvent (DES); $AlCl_3$−urea

1 Introduction

There are metals and alloys of commercial importance that are impossible to be electrochemically electrodeposited from aqueous solutions. This is due to their electrodeposition potentials in aqueous electrolytes being negative. Such metals, e.g. aluminium, have to be electrodeposited from aprotic electrolytes. Aluminium is a key prototype element for deposition studies of metals, such as Ti, Zr, Hf, V, Nb, Ta, Mo and W, for which electrodeposition from aqueous electrolytes is considered to be inadequate. Aluminium can be electrodeposited only from inorganic molten salts and organic solvents because its electrodeposition potential in aqueous electrolytes is negative, −1670 mV (vs NHE).

Inorganic molten salts, comprosed of $AlCl_3$ and inorganic salts such as NaCl, KCl, $CaCl_2$ and LiCl [1−6], have been a subject of investigation for several decades as possible electrolytes for aluminium electrodeposition. It was found that inorganic molten salts exhibit some disadvantages: narrow electrochemical windows, low dissolving capability of aluminium salt, highly corrosive nature, relatively high working temperatures, sensitivity to moisture, sensitivity to oxygen and high energy consumption [3−6].

Electrodeposition of aluminium from organic solutions is limited because of their narrow electrochemical window, substantial volatility and flammability [1,7]. Subsequently, low temperature and moisture insensitive route are key technological

---

Corresponding author: Vesna S. CVETKOVIĆ; E-mail: v.cvetkovic@ihtm.bg.ac.rs

DOI: 10.1016/S1003-6326(20)65257-8

improvement goals and aprotic ionic liquids were identified as leading candidates [1,4,8−10]. In last two decades, electrodeposition of aluminium and its alloys from ionic liquids (ILs), based on the mixture of organic and aluminium halides, has been extensively discussed in literatures [4,10−13]. These electrolytes are relatively easy to synthesize by addition of Lewis acidic $AlCl_3$ to a 1,3-dialkyl-imidazolium chloride, or alkyl-pyridinium chloride, or quaternary ammonium compound, under an inert atmosphere. Ionic liquid made of aluminium chloride and 1-ethyl-3-methylimidazolium chloride ([EMIm]Cl) has been considered as the most promising electrolyte, as it shows adjustable Lewis acidity over a wide range of $AlCl_3$ to [EMIm]Cl molar ratio [4]. Aluminium metal could be electrodeposited from such an acidic electrolyte, requiring three electron reduction of electroactive $Al_2Cl_7^-$ ions present in the ionic liquid [14]. One of the distinct features of aluminium deposition from chloroaluminate ionic liquids is the deposit microstructure (size and shape) and its dependence on the current density and/or the potential applied [4,11,12,15]. Due to the high electrochemical stability, low vapor pressure and relatively high ionic conductivity, ionic liquids appeared to be convenient media for electrodeposition of metals and alloys at relatively low temperatures (even in the range of 0−100 °C). However, ionic liquids are still partly moisture-sensitive and it has been shown recently that the morphology of the deposit is sensitive to parameters such as the nature of the Lewis acidity, cationic additives and diluents [3,4,9,16]. A new class of ionic liquids, referred to as ionic liquid analogues (ILAs), or so-called deep eutectic solvents (DESs), is formed from a mixture of a Lewis acidic metal halide and a Lewis basic ligand [17,18]. Due to their electrochemical and physical properties, reduced cost and minimal environmental impact, they have gained significant attention. ABBOTT et al [19] first reported on an ionic liquid made of $AlCl_3$ and urea (or acetamide), in which $AlCl_4^-$ anions and $[AlCl_2(\text{ligand})_n]^+$ cations were formed, with the latter being source for the aluminium being deposited [9,20,21]. Since then, several DESs formed with $AlCl_3$, have been used for aluminium electrodeposition [9,14,16,22,23]. Compared to classical ILs, the research into DESs is in its early stages, with the first work on the subject published in 2011 [20]. The main topics of ongoing research are two major application areas of DESs: DESs as alternative media for metals that are traditionally difficult to plate or process, and DESs as ecologically benign alternatives for synthesis [17,18]. Deep eutectic solvents are relatively insensitive to moisture and yet still have the properties of ionic liquids. Experiments showing that DES, with molar ratio of $AlCl_3$:urea ranging from 1:1 to 2:1 can be a suitable electrolyte for electrodeposition of aluminium at low temperatures, have been published by several authors [9,16,22,24,25]. A mixture of $AlCl_3$ and urea showed adjustable Lewis acidity which is a function of the molar ratio of $AlCl_3$ to urea. The largest disadvantage of these electrolytes is that their conductivity and viscosity are inferior to those of conventional chloroaluminate melts and ionic liquids [16−18]. The studies of electrodeposition of aluminium in the $AlCl_3$−urea DESs system indicated that aluminium deposition/dissolution is reversible [9,23,25]. Consequently, the demands for the next generation of higher energy storage systems based on rechargeable Al-ion batteries provoked intensive research to explore viable solutions and design using the $AlCl_3$−urea DESs system [24,26,27]. Despite the progress in this field, some of the issues regarding low discharge voltage, capacity or coulombic efficiency, still remain a challenge. Based on the obtained results, it can be expected in the near future that the $AlCl_3$−urea ionic liquids system, as nontoxic electrolyte, is to be suitable for rechargeable Al-ion batteries.

A great majority of the research devoted to the electrochemical deposition/dissolution of aluminium in melts, ionic liquids and deep eutectic electrolytes has been done under very rigorous control of moisture and oxygen presence in the experimental setup [3,4,8,9,18].

The aim of this work was to investigate electrodeposition of aluminium onto glassy carbon and aluminium substrates from $AlCl_3$−urea DESs system at near room temperatures, without additional purification of the chemicals used to prepare the electrolyte and without rigorous control of moisture and oxygen presence in the working space. The effects of changing temperature, working potential, controlled deposition current density and deposition time on the morphology of deposited aluminium without steering of electrolyte are to be recorded.

2 Experimental

Electrolyte preparation was initiated by adding 1.6 mol of $AlCl_3$ (used as received, >99%, Aldrich Chemical Company, Inc.) to 1 mol of urea (used as received, p.a. Carlo Erba, France) in a 50 mL glass container. The chemicals were then slowly mixed under argon atmosphere. The resulting homogeneous, yellow coloured liquid was kept at 50 °C for 30 min and then left to cool gradually to room temperature in a glove box. Finally, the electrolyte was transferred from the container to a three-electrode electrochemical cell. The cell was supplied with argon and subsequent experiments were done outside the glove box.

Two aluminium electrodes (high purity, Alfa Products, Thiokol Ventron Division, USA) were used: wire with 3 mm in diameter as the reference electrode and curved rectangular shovel with geometrical area of 15 cm^2 as the counter electrode. Cylindrical glassy carbon (GC), or aluminium, working electrode with surface area of 0.5 cm^2 was placed in the center of the cell and exposed to the ionic liquid (electrolyte). Prior to the electrochemical measurements, aluminium electrodes were polished and then etched as described previously [28−30]. Glassy carbon working electrode was polished with 0.05 μm alumina powder (Merck), cleaned by sonification in Milli-Q water in several intervals for 5 min. All electrodes were finally thoroughly washed with deionised water and absolute ethanol.

Study of the aluminium deposition/dissolution was conducted using cycling voltammetry (CV), potentiodynamic polarization curves, chronoamperometry and chronopotentiometry with an EG&G PAR 273A potentiostat/galvanostat controlled by Power Suite software (Princeton Applied Research, USA). CV was conducted using varying scan rates. Potentiostatic and galvanostatic investigations were done at three different temperatures: 25, 35 and 50 °C. During deposition, the electrolyte was not stirred. After deposition, samples were rinsed with absolute ethanol to remove any residue of the ionic liquid and left to dry in air before characterization. The microstructures of the deposits were recorded using scanning electron microscope (SEM, TESCAN digital microscope; model VEGA3, Brno, Czech Republic) and chemical composition of the deposit was analysed by energy dispersive spectroscopy (EDS, Oxford INCA, 3.2, UK). The deposit obtained by potentiostatic electrodeposition at −250 mV vs. Al and 50 °C, was collected from GC working electrode, and analysed by X-ray diffraction (XRD) measurements on Philips PW 1050 powder diffractometer at room temperature with Ni filtered Cu K_α radiation (λ=1.54178 Å), scintillation detector within 2θ range of 15°−75° in steps of 0.05°, and scanning time of 5 s per step.

3 Results and discussion

3.1 Glassy carbon substrate

Typical cyclic voltammograms of aluminium deposition/dissolution recorded on GC electrode in $AlCl_3$−urea (molar ratio of 1.6:1) ionic liquid are shown in Fig. 1. They generally resemble those on Cu [22], GC, Pt, Al [9,16,25], W [23] obtained with similar electrolytes and working temperatures. The potential of working electrode was scanned from initial potential, φ_i=1400 mV vs. Al (slightly negative to the working electrode reversible potential), towards the final chosen negative potentials, φ_f, and back with a scan rate of 10 mV/s. In the aluminium underpotential region, two reduction current waves were recognized: one with the peak potential at about 600 mV vs. Al (Wave A), and the other with the peak potential at about 300 mV vs. Al (Wave B) (Fig. 1(a)). Their maximum current densities were below 35 μA/cm^2. The waves, A and B, did not show oxidation counterparts and cannot be attributed to aluminium underpotential deposition. Their peak potentials did not change substantially when temperature of the system was increased from 25 to 35 and 50 °C. Similar current waves were reported in the literature, but no decisive identification was offered. Some authors concluded that waves A and B are related to Cl^- ion reductive desorption [31], and others however considered possibility of urea adsorption being responsible for those waves [32]. Latter, it was suggested [4] that the organic cation component is reduced at more positive potentials than $AlCl_4^-$ cation.

At lower overpotential, the charges under the cathodic (C) and anodic current wave (C′) were approximately the same in size, indicating relatively good reversibility of Al deposition and dissolution under the conditions examined. At higher overpotential (Fig. 1(b)), the charge under the cathodic current waves became somewhat greater than the anodic charge. The increase in the deposition charge resulted in the anodic maximum peak potentials being moved toward more anodic values and tentative appearance of the additional small current wave integrated into the original, larger one.

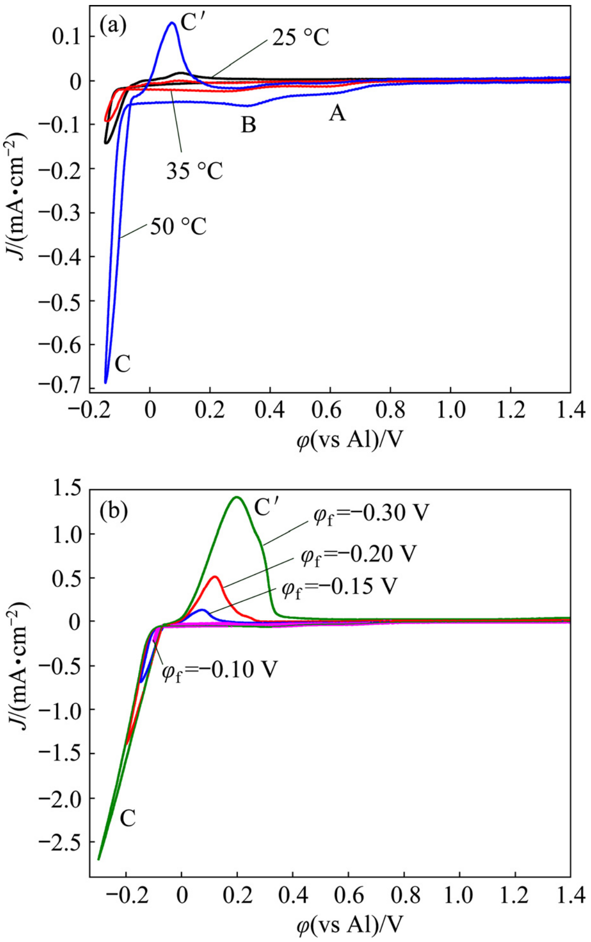

Fig. 1 Cycling voltammograms recorded on GC electrode with v=10 mV/s: (a) φ_i=1400 mV vs. Al and φ_f=−150 mV vs. Al at different temperatures; (b) φ_i= 1400 mV vs. Al to different φ_f values, at T=50 °C

The peak currents of the cathodic and anodic waves, recorded within the same potential limits and sweep rates, increased by almost ten times when the working temperature was changed from 25 to 50 °C, as shown in Fig. 1(a). Cathodic section of the voltammograms recorded suggested that aluminium deposition starts at the potential of about −120 mV vs. Al, at all temperatures used.

The onset overpotential of aluminium deposition onto GC recorded was lower than that on any other substrate published in the literature available. It appears that additives to the electrolyte [9,16,22,23,25], like decane (to prevent moisture affecting the electrolyte), or Li-halides and toluene (to improve conductivity), did not substantially increase the deposition current densities nor decrease the starting deposition potentials compared to those obtained with the original $AlCl_3$−urea electrolyte used. However, it should be concluded that an $AlCl_3$:urea molar ratio higher than 1.3:1 is needed for successful Al deposition.

Two ionic species dominate in the used electrolyte and they are a product of the possible reaction in the $AlCl_3$−urea system proposed as [9,20,26,33]

$$n\text{Urea}+\text{AlCl}_3\rightarrow[\text{AlCl}_2\cdot n(\text{Urea})]^{+}+\text{AlCl}_4^{-} \tag{1}$$

where n is coordination number of urea controlled by the mole ratio of $AlCl_3$ to urea, and $[AlCl_2\cdot n(Urea)]^+$ is the cationic species which is reduced to aluminium at the cathode.

Examples of the current density−time responses to potential steps applied to the GC working electrode in the given electrolyte at three different temperatures are given in Fig. 2, and those recorded at a chosen temperature but different potentials applied are shown in Fig. 3. J−t transients obtained with the same aluminium overpotential applied at three different temperatures revealed that temperature does not substantially influence the onset aluminium deposition overpotential. It seemed to be always between −105 and −110 mV vs. Al under the condition of the experiments. However, further investigation of the potentiostatic aluminium deposition done at the same temperature showed that the onset aluminium deposition potential was closer to −95 mV vs. Al (Fig. 3(b)).

The initial rising segments of the J−t transients are recorded (Fig. 2(a)), according to the criteria given in the literatures [34,35] as

$$J=\frac{2zF\pi M^2N_0k^3t^2}{\rho^2} \tag{2}$$

where z is number of electrons exchanged, F is Faraday constant, M is molecular mass of the deposited materials, N_0 is total number of nucleation sites, k is growth rate constant, t is time,

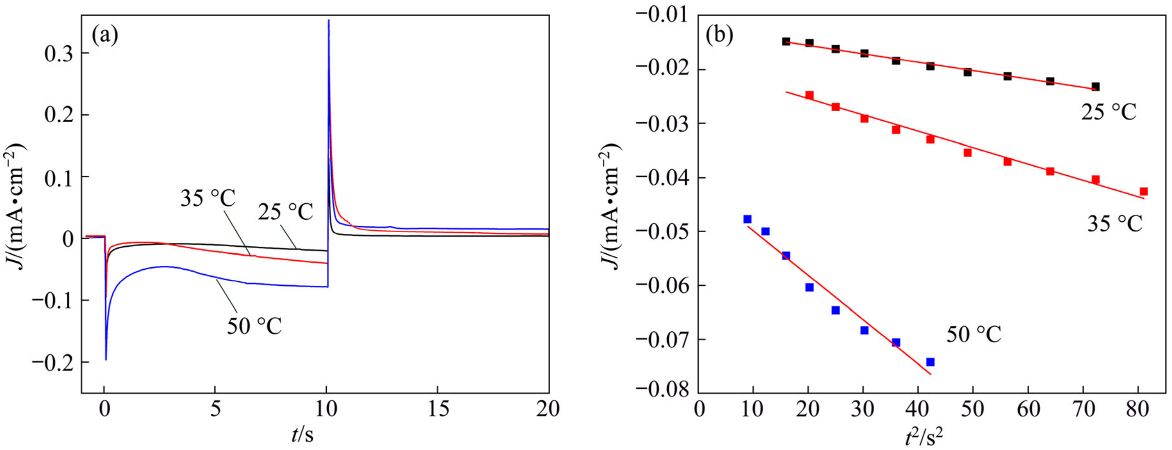

Fig. 2 Current density−time transients recorded on GC electrode at different temperatures with cathodic overpotential applied φ_f=−110 mV vs. Al (a) and $J=f(t^2)$ plots (b) obtained from $J-t$ transients in Fig. 2(a)

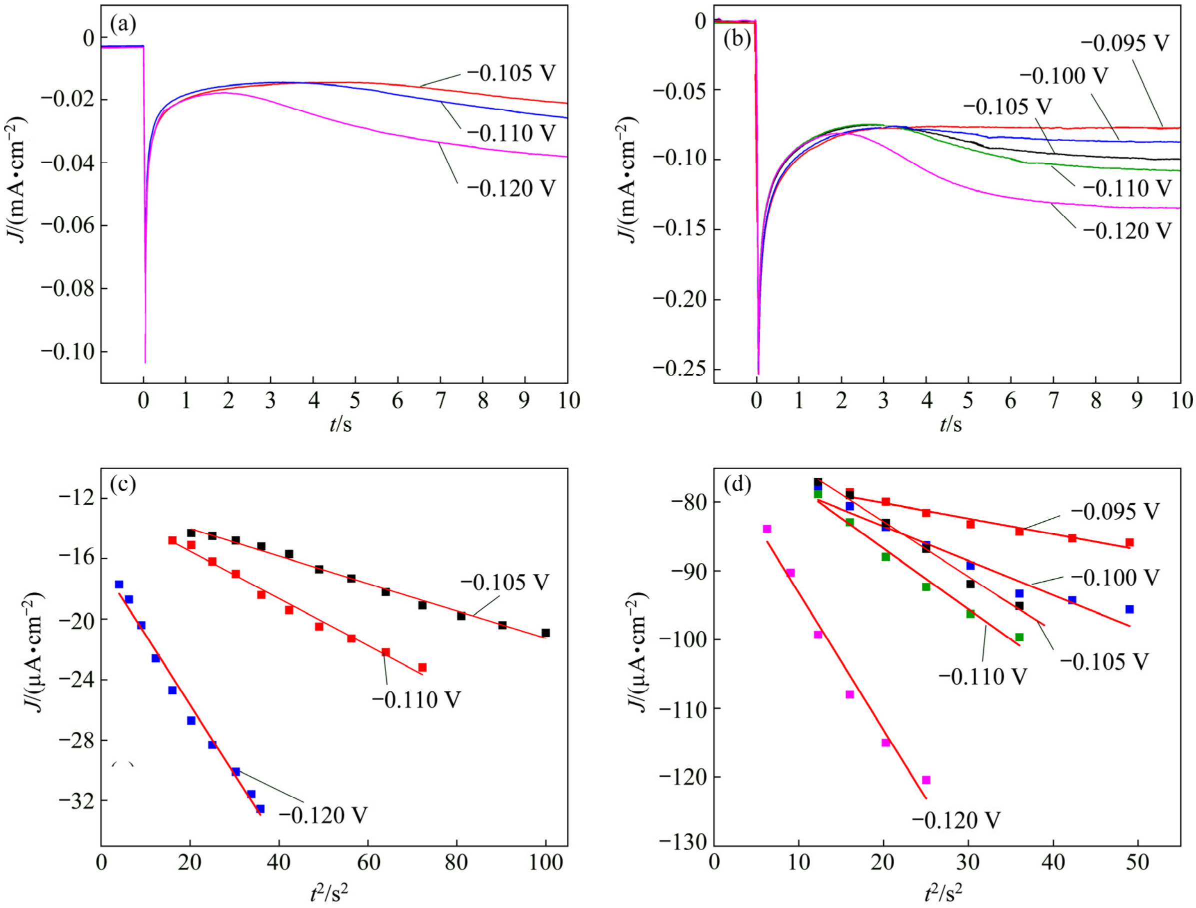

Fig. 3 Current density−time transients recorded on GC electrode with different cathodic overpotentials applied: (a) T=25 °C; (b) T=50 °C; (c) $J=f(t^2)$ plot obtained from (a); (d) $J=f(t^2)$ plot obtained from (b)

and ρ is specific density of the deposited material. It is shown that aluminium deposition onto GC from the electrolyte used and at the temperatures applied started and proceeded by instantaneous three-dimensional nucleation and growth (Fig. 2(b)).

Furthermore, $J-t$ transients revealed that the deposition current density, obtained with the same overpotential applied, increased several times with increased operating temperature (e.g. from about 0.01 to about 0.10 mA/cm^2 for temperature increase from 25 to 50 °C, as shown in Fig. 2(a)). Apparently, this should be ascribed to the increase of the electrolyte conductivity and the decrease of the viscosity [16].

SEM micrographs and EDS analysis of the aluminium deposited onto GC by the potentiostatic method at two different temperatures are presented in Figs. 4 and 5. Even with longer deposition time and higher temperature (50 °C) used, the deposit did not fully cover the whole substrate in the form of a layer. Instead, it appeared as families of grains of different sizes and shapes. The grains on the surface of GC increased with deposition time and temperature (Figs. 4(b) and 5(b, c)). Further increase in the deposition overpotential led to expected current increase. However, once the overpotential exceeded −220 mV vs. Al, there were indications of current density reaching a limit at longer deposition time applied, even at the temperature of 50 °C. Deposition at overpotential

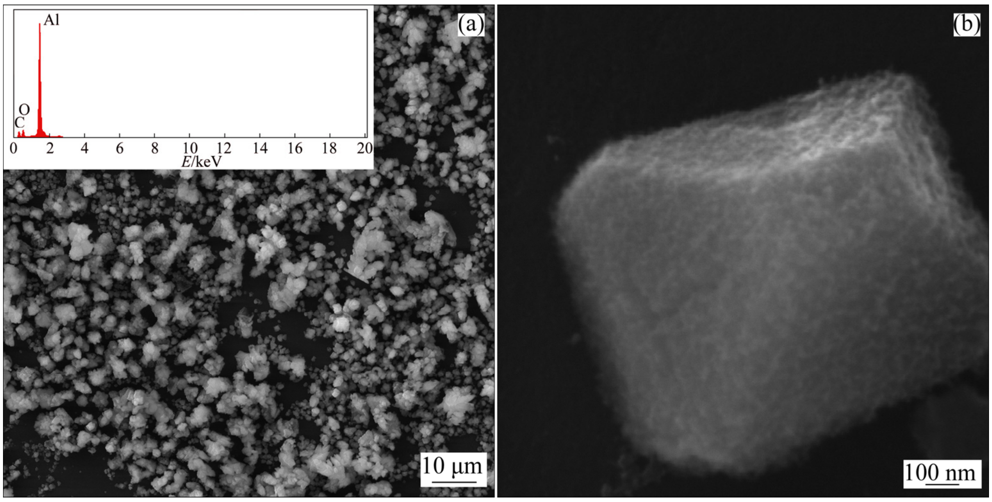

Fig. 4 SEM images of aluminium deposits obtained at 25 °C on GC by potentiostatic regimes at −200 mV vs. Al, for 30 min

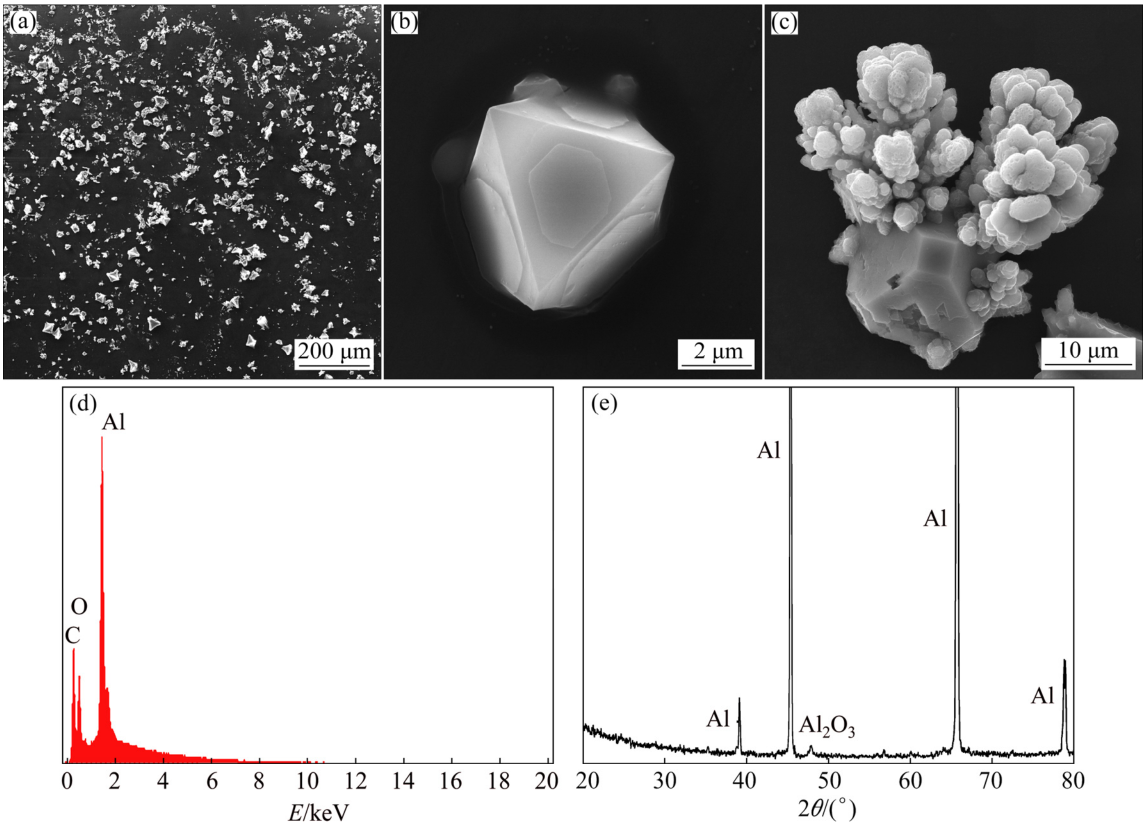

Fig. 5 SEM images of aluminium deposits obtained at 50 °C on GC by potentiostatic regimes at −250 mV vs. Al: (a, b) For 30 min; (c) For 50 min; (d) EDS analysis of sample from (a); (e) XRD pattern of deposit obtained on GC after 3 h of deposition

exceeding −250 mV vs. Al and deposition time of 30 min led to transformation of initially crystalographically regular grain shapes (see Fig. 4(b) or Fig. 5(b)) into morphologies characteristic of diffusion controlled deposition (see Fig. 5(c)). EDS spectra of the deposits identified only aluminium on the GC substrate.

The XRD analysis made of the deposit obtained on GC potentiostatically by long time deposition showed only aluminium being deposited as presented in Fig. 5(e). Apart from Al [JCPDS No: 03-065-2869], trace of Al_2O_3 [JCPDS No: 00-011-0517] could be detected because it was not possible to handle sample without exposing it to the atmosphere.

Variation of electrode potential during galvanostatic deposition of aluminium on GC at different temperatures is shown in Fig. 6(a). Photographs of the aluminium electrodeposited at current density of −2 mA/cm^2 and 50 °C are shown in Figs. 6(b−e). Applying the chronopotentiostatic regime showed that the deposition current density of −2 mA/cm^2 demanded a relatively high working electrode potential, which decreased dramatically with the increase in working temperature from 25 to 50 °C (Fig. 6(a)). These findings are in accordance with the propositions [14] that temperature has strong influence on the electrolyte conductivity and viscosity. EDS recordings show only aluminium as the deposit on the GC cathode. The deposit was made of families as well as individual grains, some having very regular crystalline shape of 2−5 μm in size (Fig. 6(b)), and some being enriched by very elaborate three-dimensional additions (tree-like, grape-like, flakes-like, etc) to the original grains (Figs. 6(c, d)).

3.2 Aluminium substrate

Voltammograms of aluminium deposition/dissolution (Fig. 7), recorded on aluminium working electrode, in the electrolyte used and potential range between 700 mV vs. Al and −300 mV vs. Al, displayed a reversible aluminium deposition and dissolution. The potential was changed from initial potential, φ_i, to cathodic end potential, φ_c, then to anodic end potential, φ_a, and back to φ_f being the reversible potential. The charges recorded under cathodic current waves and anodic counterparts were close, although the latter were somewhat lower in value. Similar conclusions can be found in the works where electrolytes consisted of aluminium chloride, urea and additives used [9,23]. Here again, the substantial increase in maximum peak current density for the same potential applied was recorded when the temperature was changed from 25 to 50 °C. In other words, the voltammograms of Al deposition/dissolution on Al substrate appeared to be very similar to those recorded on GC working electrodes in the same system and under the same conditions.

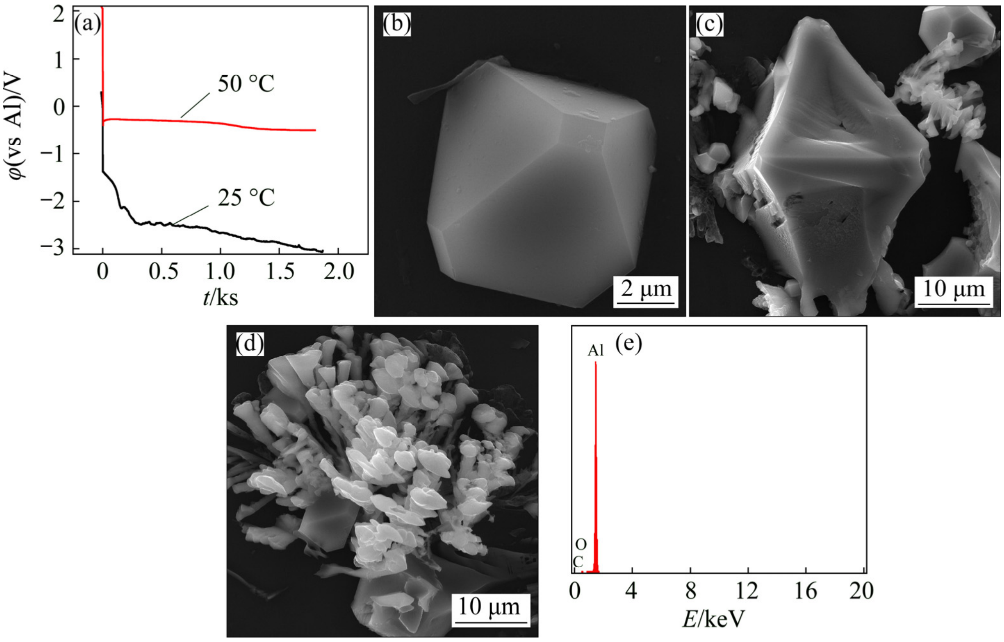

Fig. 6 Galvanostatic regimes applied for aluminium deposition at −2 mA/cm^2 for 30 min (a), SEM images of aluminium deposits obtained on GC at 50 °C (b−d), and EDS result (e) from sample in (b)

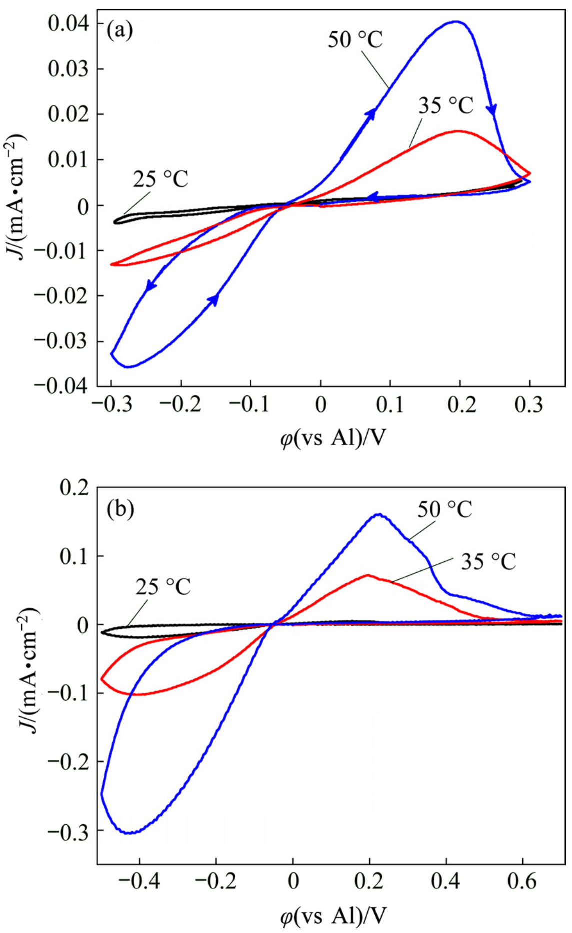

Fig. 7 Cycling voltammograms recorded on Al electrode from $AlCl_3$−urea at different temperature (v=10 mV/s): (a) φ_i=0 mV; φ_c=−300 mV, φ_a=300 mV and φ_f=0 mV (vs Al); (b) φ_i=0 mV, φ_c=−500 mV, φ_a=700 mV and φ_f= 0 mV (vs Al)

Examples of current density−time responses to the potential applied onto the aluminium working electrodes at different temperatures and at one temperature but different potentials are given in Figs. 8(a) and (b), respectively. The J−t transients obtained appeared to be somewhat different from those obtained on GC under the same conditions. Nevertheless, the analysis of the initial rising segments of the deposition J−t transients indicated linearity of J=f(t^2) (Fig. 8(c)), characteristic of instantaneous 3D nucleation and growth, as given in Eq. (2) [34,35], independent of temperature applied. The deposition current densities recorded for the same potential applied increased by 4−5 times with the temperature changed from 25 to 50 °C (Figs. 8(a) and (b)).

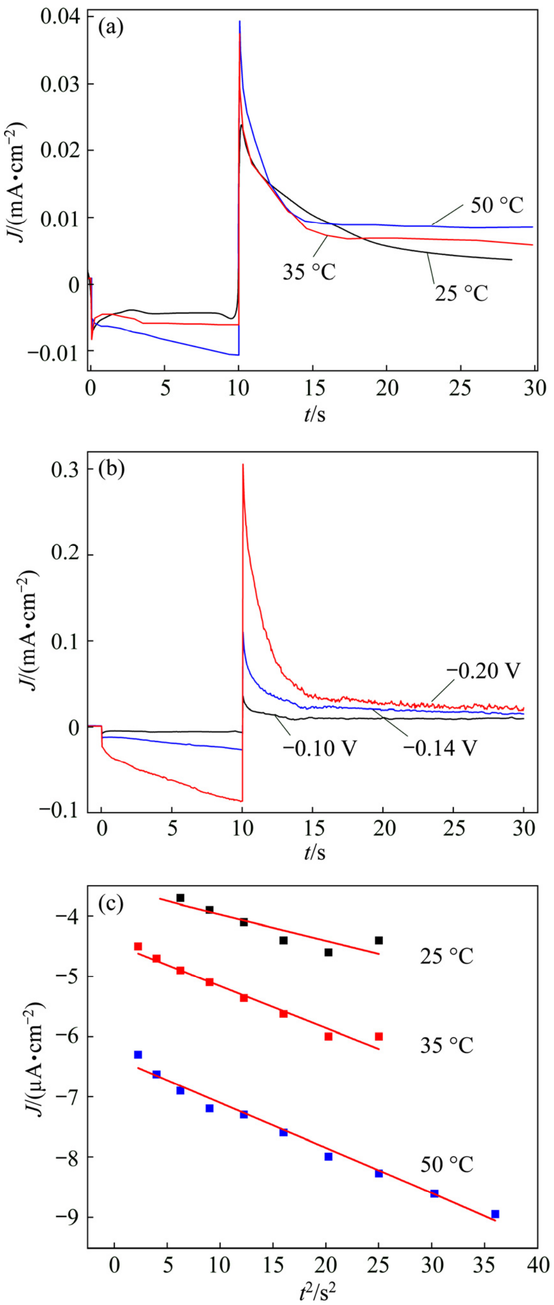

Fig. 8 Current density−time transients recorded on Al electrode from $AlCl_3$−urea: (a) At different temperatures and constant overpotential φ_c=−100 mV and φ_a=100 mV (vs Al); (b) At 50 °C and different cathodic overpotentials; (c) J=f(t^2) derived from (a)

In addition, the current densities recorded for the same deposition overpotential and temperature applied did not differ significantly from those recorded for GC under the same conditions (see Figs. 2 and 3). The current density responses to the potentiostatic regimes, (overpotentials up to −500 mV vs. Al), on both GC and aluminium substrates, were in the range between 0.01 and 0.1 mA/cm^2 when the working temperature was between 25 and 50 °C.

Aluminium deposits on aluminium substrate obtained by potentiostatic deposition at different temperatures recorded by SEM and analysed by EDS are presented in Figs. 9 and 10. It was found that the grain size and the shape of the aluminium deposited onto aluminium electrode, obtained under the same or very similar conditions (electrolyte, potential and temperature), differed from those obtained by aluminium deposition onto GC. For example, at the overpotentials larger than −220 mV vs. Al, the grain distribution became denser, and during 30 min the shape of the grains changed from

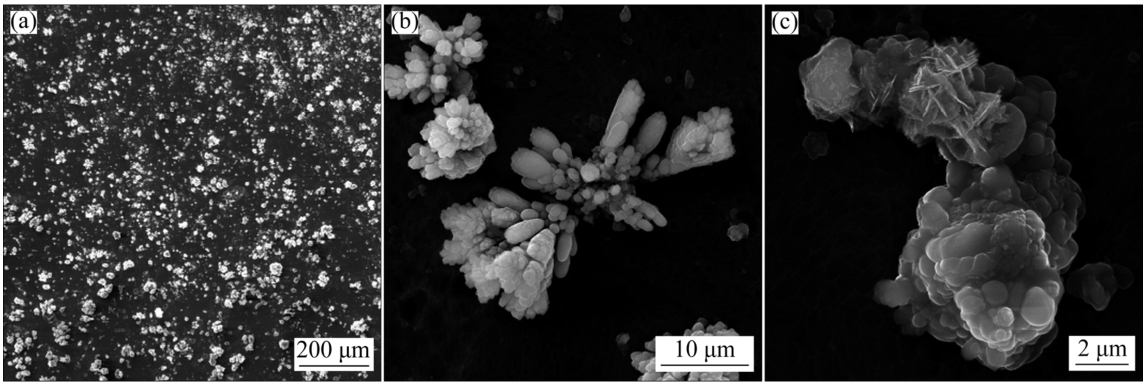

Fig. 9 SEM images of Al deposits obtained on Al substrate by potentiostatic deposition φ_c=−220 mV (vs Al) for 30 min at 50 °C

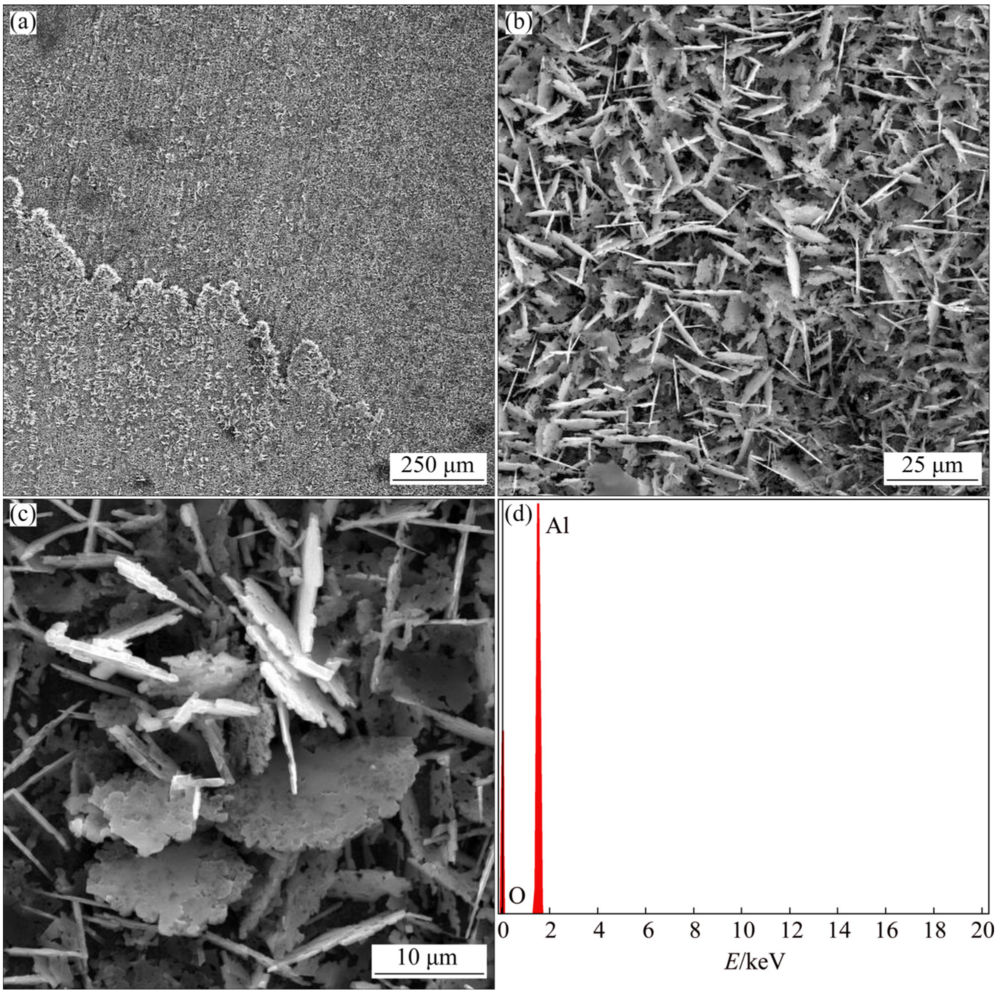

Fig. 10 Aluminium deposits obtained on aluminium by potentiostatic regime φ_c=−250 mV (vs Al) for 30 min at 35 °C: (a, b, c) SEM images; (d) EDS result from sample in (b)

crystalline boulders and nodular grains to a very complex and irregular ones (Fig. 9). SEM images show that the coverage of aluminium substrate was consequently higher compared to GC substrate, even at somewhat smaller deposition overpotentials (Figs. 5 and 9). After 30 min of deposition, at potentials equal and more negative than −250 mV vs. Al and 35° C, Al deposit of very high specific surface area covering the aluminium substrate was recorded. It seemed as if it was made of two layers, the bottom one being made of smaller flake-like grains (Fig. 10(a)), and the second one made of bigger flake shapes (Figs. 10(b, c)). Aluminium was detected as the only element in the deposits by EDS analysis (Fig. 10(d)). There are records of similar morphology of Al deposit on Cu and Cu/Al alloy obtained under somewhat different conditions and certainly different composition of the electrolyte used [22,25,36].

Change in the working potential with time as a result of extended galvanostatic aluminium deposition onto aluminium substrate is presented in Fig. 11. The applied deposition current density of −2 mA/cm^2 provoked cathodic overpotential in the range from −600 to −1800 mV vs. Al when working temperature was changed in the sequence of 25, 35 and 50 °C.

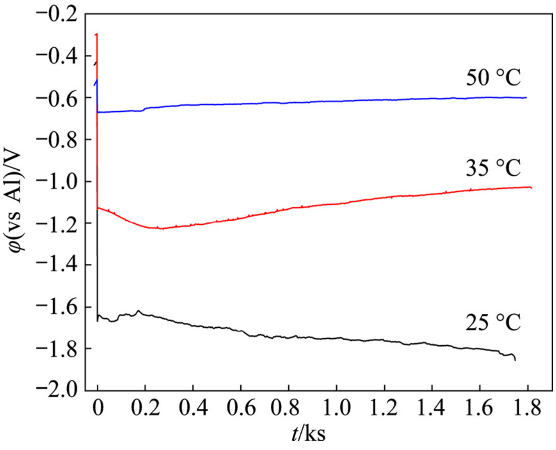

Fig. 11 Potential−time responses to galvanostatic deposition of aluminium onto aluminium from used electrolyte at different temperatures (−2 mA/cm^2, 30 min)

The difference in appearance of aluminium deposits (grain surface density, shape and size), obtained under the same conditions on GC and aluminium substrate was reiterated in the examples of galvanostatic aluminium deposition onto aluminium electrode, as shown in Fig. 12. The reasons for this finding are not absolutely clear at this stage of our investigation.

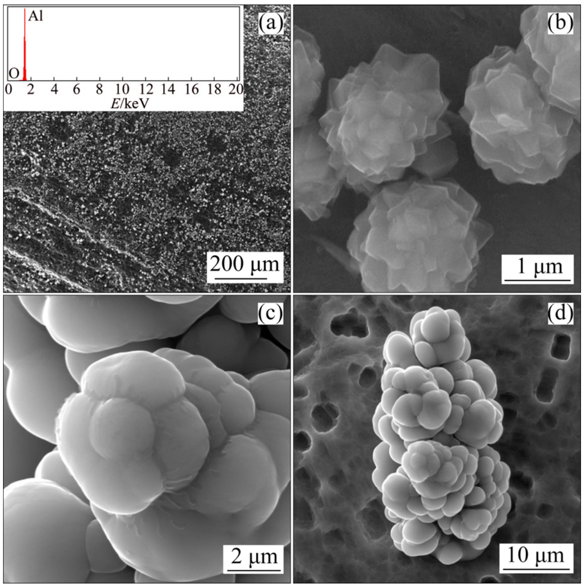

Fig. 12 SEM images of aluminium deposits onto aluminium substrate obtained by galvanostatic regime of −2 mA/cm^2: (a) Morphology with embedded EDS; (b) T=35 °C; (c, d) T=50 °C

However, it was apparent again that a uniform Al deposit layer could not be put down onto the Al substrate under the experimental conditions described. Instead, aluminium deposits consisting of great number of crystallites of various shapes and very small individual sizes were obtained.

4 Conclusions

(1) Aluminium was electrodeposited from the deep eutectic system $AlCl_3$:urea=1.6:1 (prepared from chemicals as-received without additional purification) onto glassy carbon and aluminium at temperatures ranging from 25 to 50 °C. The experiments under potentiostatic and galvanostatic regimes were done in the electrochemical cell outside a glovebox in the absence of electrolyte stirring.

(2) On glassy carbon and aluminium surfaces, Al deposition started at about −95 mV vs. Al as 3D instantaneous nucleation and growth. Deposition lasting for 30−60 min did not produce a uniform aluminium layer on either substrate, irrespective of changes in working temperature. Instead, individual grain populations of deposits with highly-developed specific surface area were recorded. The size (from

nanometer to micrometer) and shape of the Al grains depended on the potential, current density and temperature applied. The higher the deposition overpotential, irrespective of temperature, the higher the probability of regular crystal grains and boulders being deformed and needle-like and flake-like grains were formed. At potentials above −250 mV vs. Al, complicated grain morphology including needle-like and flake-like structures became the dominant forms.

(3) It was observed that the aluminium dissolution processes, when recorded as counterparts to the deposition ones, were comparatively slower and this should be attributed to the slow re-entrance of the Al^{3+} ions into the complexes made originally of urea and $AlCl_3$. This suggests that it is the number of ligands that is important in dissolution processes rather than the Al^{3+} ions mass transport and otherwise very low conductivity of the electrolyte.

Acknowledgments

This work was supported by the Ministry of Education, Science and Technological Development of the Republic of Serbia (Grant No. 172060).

References

[1] FALOLA B D, SUNI I I. Low temperature electrochemical deposition of highly active elements [J]. Current Opinion in Solid State Materials Science, 2015, 19: 77−84.

[2] STAFFORD G R, HUSSEY C L. Advances in electrochemical science and engineering [M]. Vol. 8. New York: Weinheim: Wiley-VCH Verlag GmbH, 2001: 275−348.

[3] SIMKA W, PUSZCZYK D, NAWRAT G. Electrodeposition of metals from non-aqueous solutions [J]. Electrochimica Acta, 2009, 54: 5307−5319.

[4] TSUDA T, STAFFORD G R, HUSSEY C L. Review—Electrochemical surface finishing and energy storage technology with room-temperature haloaluminate ionic liquids and mixtures [J]. Journal of The Electrochemical Society, 2017, 164: H5007−H5017.

[5] UEDA M. Overview over studies of electrodeposition of Al or Al alloys from low temperature chloroaluminate molten salts [J]. Journal of Solid State Electrochemistry, 2017, 21: 641−647.

[6] KAN Hong-min, WANG Zhao-wen, WANG Xiao-yang, ZHANG Ning, Electrochemical deposition of aluminum on W electrode from $AlCl_3$–NaCl melts [J]. Transactions of Nonferrous Metals Society of China, 2010, 20: 158−164.

[7] MIYAKE M, KUBO Y, HIRATO T. Hull cell tests for evaluating the effects of polyethylene amines as brighteners in the electrodeposition of aluminum from dimethylsulfone–$AlCl_3$ baths [J]. Electrochimica Acta, 2014, 120: 423−428.

[8] ABBOTT A P, FRISCH G, RYDER K S. Electroplating using ionic liquids [J]. Annual Review of Materials Research, 2013, 43: 335−358.

[9] ABBOTT A P, HARRIS R C, HSIEH Y T, RYDER K S, SUN I W. Aluminium electrodeposition under ambient conditions [J]. Physical Chemistry Chemical Physics, 2014, 16: 14675−14681.

[10] ZHANG Li-peng, YU Xian-jin, DONG Yun-hui, LI De-gang, ZHANG Ya-li, LI Zhong-fang. Electrodeposition of aluminum on magnesium from ionic liquid (EMIM)Br–$AlCl_3$ [J]. Transactions of Nonferrous Metals Society of China, 2010, 20: s245−s248.

[11] JIANG T, CHOLLIER BRYM M J, DUBE G, LASIA A, BRISARD G M. Electrodeposition of aluminium from ionic liquids. Part I: Electrodeposition and surface morphology of aluminium from aluminium chloride ($AlCl_3$)–1-ethyl-3-methylimidazolium chloride ([EMIm]Cl) ionic liquids [J]. Surface and Coatings Technology, 2006, 201: 1−9.

[12] JIANG T, CHOLLIER BRYM M J, DUBE G, LASIA A, BRISARD G M. Electrodeposition of aluminium from ionic liquids. Part II: Studies on the electrodeposition of aluminum from aluminum chloride ($AICl_3$)-trimethylphenylammonium chloride (TMPAC) ionic liquids [J]. Surface and Coatings Technology, 2006, 201: 10−18.

[13] LEE Jae-joon, BAE In-tae, SCHERSON D A, MILLER B, WHEELER K A. Underpotential deposition of aluminum and alloy formation on polycrystalline gold electrodes from $AlCl_3$/EMIC room-temperature molten salts [J]. Journal of The Electrochemical Society, 2000, 147: 562−566.

[14] LI Min, GAO Bing-liang, LIU Cheng-yuan, CHEN Wen-ting, WANG Zhao-wen, SHI Zhong-ning, HU Xian-wei. $AlCl_3$/amide ionic liquids for electrodeposition of aluminum [J]. Journal of Solid State Electrochemistry, 2016, 21: 469−476.

[15] SUN Wen-cheng, HAN Xiao-fei, TAO Meng. Electroplating of aluminium on silicon in an ionic liquid [J]. ECS Electrochemistry Letters, 2015, 4: D5−D7.

[16] PRABU S, WANG Hong-wen. Factors affecting the electrodeposition of aluminum metal in an aluminum chloride–urea electrolyte solution [J]. Journal of The Chinese Chemical Society, 2017, 64: 1467−1477.

[17] ZHANG Q, VIGIER K D O, ROYER S, JEROME F. Deep eutectic solvents: Syntheses, properties and applications [J]. Chemical Society Reviews, 2012, 41: 7108−7146.

[18] SMITH E L, ABBOTT A P, RYDER K S. Deep eutectic solvents (DESs) and their applications [J]. Chemical Reviews, 2014, 114: 11060−11082.

[19] ABBOTT A P, CAPPER G, DAVIES D L, RASHEED R K, TAMBYRAJAH V. Novel solvent properties of choline cholride urea mixtures [J]. Chemical Communications, 2003: 70−71.

[20] ABOOD H M A, ABBOTT A P, BALLANTYNE A D, RYDER K S. Do all ionic liquids need organic cations? Characterisation of $[AlCl_2\cdot n\text{Amide}]^+AlCl_4^-$ and comparison with imidazolium based systems [J]. Chemical Communications, 2011, 47: 3523−3525.

[21] ABBOTT A P, McKENZIE K J. Application of ionic liquids to the electrodeposition of metals [J]. Physical Chemistry Chemical Physics, 2006, 8: 4265−4279.

[22] ABOOD H M A, DAWOOD N L. Morphology of electrodeposited aluminium metal from aluminium chloride-urea room temperature ionic liquid (RTIL) at variable parameters [J]. International Journal of Science and Research, 2015, 4: 753−760.

[23] LI Min, GAO Bing-liang, CHEN Wen-ting, LIU Cheng-yuan, WANG Zhao-wen, SHI Zhong-ning, HU Xian-wei. Electrodeposition behavior of aluminum from urea−acetamide−lithium halide low-temperature molten salts [J]. Electrochimica Acta, 2015, 185: 148−155.

[24] ANGELL M, PAN Chun-jern, RONG You-min, YUAN Chun-ze, LIN Meng-chang, HWANG Bing-joe, DAI Hong-jie. High coulombic efficiency aluminum-ion battery using an $AlCl_3$−urea ionic liquid analog electrolyte [J]. Proceedings of the National Academy of Science of the USA, 2017, 114: 834−839.

[25] TSUDA T, MIYAKAWA R, KONDA A, IKEDA Y, KUWABATA S. Aluminum nanoplatelets electrochemically produced in lewis acidic $AlCl_3$–urea solvate ionic liquids [C]//69th Annual Meeting of the International Society of Electrochemistry. Bologna, Italy: ISE, 2018: 59.

[26] JIAO Han-dong, WANG Chen, TU Ji-guo, TIAN Dong-hua, JIAO Shu-qiang. A rechargeable Al-ion battery: Al/molten $AlCl_3$−urea/graphite [J]. Chemical Communications, 2017, 53: 2331−2334.

[27] LI Jun-feng, TU Ji-guo, JIAO Han-dong, WANG Chen, JIAO Shu-qiang. Ternary $AlCl_3$−urea−[EMIm]Cl ionic liquid electrolyte for rechargeable aluminum-ion batteries [J]. Journal of The Electrochemical Society, 2017, 164: A3093−A3100.

[28] JOVIĆ V D, JOVIĆEVIĆ J N. Aluminium electrodeposition from $AlCl_3$−NaCl melts on glassy carbon, platinum and gold electrodes [J]. Journal of Applied Electrochemistry, 1989, 19: 275−280.

[29] RADOVIC B S, RDWARDS R A H, JOVIĆEVIĆ J N. Aluminium underpotential deposition from $AlCl_3$+NaCl melts on gold electrodes [J]. Journal of Electroanalytical Chemistry, 1997, 428: 113−121.

[30] JOVIĆEVIĆ N, CVETKOVIĆ V S, KAMBEROVIĆ Ž J, JOVIĆEVIĆ J N. Al−Cd alloy formation by aluminum underpotential deposition from $AlCl_3$+NaCl melts on cadmium substrate [J]. Metallurgical and Materials Transactions B, 2013, 44: 106−114.

[31] BUČKO M, CULLITON D, BETTS A J, BAJAT J B. The electrochemical deposition of Zn−Mn coating from choline chloride–urea deep eutectic solvent [J]. Transaction of the Institute of Metal Finishing, 2017, 95: 60−64.

[32] GOMEZ E, VALLES E. Platinum electrodeposition in an ionic liquid analogue: Solvent stability monitoring [J]. International Journal of Electrochemical Science, 2013, 8: 1443−1458.

[33] ABOOD H M A, FADHIL M H. Investigation of Lewis acid-base reaction of acidic species present in aluminum chloride-urea ionic liquid [J]. Journal of Al-Nahrain University, 2014, 17: 71−75.

[34] FLEISCHMANN M, THIRSK H R. Advances in electrochemistry and electrochemical engineering [M]. Vol 3. New York: Interscience, 1963: 168−173.

[35] GUNAWARDENA G, HILLS G, MONTENEGRO I, SCHARIFKER B. Electrochemical nucleation: Part I. General consideration [J]. Journal of Electroanalytical Chemistry and Interfacial Electrochemistry, 1982, 138: 225−239.

[36] PRADHAN D, REDDY R G. Dendrite-free aluminum electrodeposition from $AlCl_3$-1-ethyl-3-methyl-imidazolium chloride ionic liquid electrolytes [J]. Metallurgical and Materials Transaction B, 2012, 43: 519−531.

室温及非传统条件下 $AlCl_3$−尿素低共熔溶剂中铝的电沉积

Vesna S. CVETKOVIĆ[1], Nataša M. VUKIĆEVIĆ[1], Niko JOVIĆEVIĆ[2],
Jasmina S. STEVANOVIĆ[1], Jovan N. JOVIĆEVIĆ[1]

1. Institute of Chemistry, Technology and Metallurgy, National Institute,
Department of Electrochemistry, University of Belgrade, Belgrade, Serbia;
2. Nissan Technical Center North America, Inc., 39001 Sunrise Drive, Farmington Hills, MI 48331-3487, USA

摘　要：研究在接近室温下 $AlCl_3$−尿素低共熔溶剂(DESs)体系中铝在玻璃碳和铝基底上的电沉积，而不需要对用于制备电解质的化学试剂进行额外的净化处理，也没有严格控制工作场所中的水分和氧气。研究改变温度、工作电势、受控沉积电流密度和沉积时间对在不搅拌电解质情况下沉积铝的形貌的影响。采用恒电势和恒电流技术，25~50 °C 下，在低共熔溶剂($n(AlCl_3):n(Urea)=1.6:1$)中将铝电沉积到玻璃状碳和铝基底上。利用 SEM、EDS 和 XRD 技术对两种基底进行研究，证实在恒电势和恒电流两种情形下均存在铝沉积物。所沉积的 Al 晶粒的形状和尺寸取决于沉积时间，尺寸从纳米级到微米级，形状从规则晶体到针状和片状结构。

关键词：铝；电沉积；低共熔溶剂(DES)；$AlCl_3$−尿素

(Edited by Bing YANG)